

Search for High Mass Resonances Decaying to Muon Pairs in $\sqrt{s} = 1.96$ TeV $p\bar{p}$ Collisions

(Dated: July 16, 2018)

We present a search for a new narrow, spin-1, high mass resonance decaying to $\mu^+\mu^- + X$, using a matrix element based likelihood and a simultaneous measurement of the resonance mass and production rate. In data with 4.6 fb^{-1} of integrated luminosity collected by the CDF detector in $p\bar{p}$ collisions at $\sqrt{s} = 1960 \text{ GeV}$, the most likely signal cross section is consistent with zero at 16% confidence level. We therefore do not observe evidence for a high mass resonance, and place limits on models predicting spin-1 resonances, including $M > 1071 \text{ GeV}/c^2$ at 95% confidence level for a Z' boson with the same couplings to fermions as the Z boson.

??

We report a search for a narrow spin-1 resonance (Z') with decays to muon pairs and a mass between $130 \text{ GeV}/c^2$ and $\approx 1 \text{ TeV}/c^2$. Such a resonance is predicted generically in models with additional gauge groups [langacker], a feature of many extensions to the standard model of particle physics (SM). Typical examples are Little Higgs models [littlehiggs] and the next-to-minimal supersymmetric model [nmssm].

Current 95% confidence level (CL) lower limits on the mass of a Z' boson with the same couplings to fermions as the Z boson (Z'_{SM}) are $1030 \text{ GeV}/c^2$ from a search of CDF dimuon data with 2.3 fb^{-1} of integrated luminosity [zprimetemp], and $1023 \text{ GeV}/c^2$ [d0ee] and $963 \text{ GeV}/c^2$ [cdf] from respective searches in dielectron data from D0 in 5.4 fb^{-1} and from CDF in 2.5 fb^{-1} , respectively.

This Letter reports a new search of the CDF dimuon data with several significant enhancements: twice the integrated luminosity, a matrix element based likelihood providing an approximately 20% relative increase in cross section sensitivity at large Z' mass, and a new statistical approach designed to maximize simultaneously both discovery potential and mass exclusion limits in searches for new physics. This new approach directly fits the data to a single Z' boson hypothesis in the plane of boson mass and signal cross section, and can be applied to any search for a hypothetical new particle of unknown mass.

We use a data sample corresponding to an integrated luminosity of 4.6 fb^{-1} , collected with the CDF II detector [cdf], a general purpose detector designed to study $p\bar{p}$ collisions at the Fermilab Tevatron. The tracking system consists of a cylindrical open-cell drift chamber and silicon microstrip detectors in a 1.4 T magnetic field parallel to the beam axis. The silicon detectors provide tracking information for pseudora-

pidity $2010 < \eta < 2.4$ for pseudorapidity and are used to reconstruct collision and decay points. The drift chamber surrounds the silicon detectors and gives full coverage in the central pseudorapidity region ($|\eta| < 1$). For the muon kinematics relevant to this search, the tracker provides an invariant mass resolution of $\delta M/M^2 \approx 0.17\%/\text{TeV}/c^2$. Electromagnetic and hadronic calorimeters surrounding the tracking system measure energy from particle showers and minimum ionizing particles such as muons. Drift chambers and scintillators located outside the calorimeters detect muons in the central pseudorapidity region $|\eta| < 1$.

Events used for this search are selected online with a trigger requiring a muon candidate with $p_T > 18 \text{ GeV}/c$. The event selection is unchanged from the previous search [zprimetemp], requiring at least two oppositely charged muons with $p_T > 30 \text{ GeV}/c$ and no identified cosmic rays [cosmics]. Each muon is required to have calorimeter deposits consistent with a minimum ionizing particle and have a track fully within the fiducial volume of the drift chamber. At least one muon must have an associated muon-chamber track.

The dominant and irreducible background is standard model Z/γ^* production with subsequent decay to muons. We model this background using events generated at leading order by PYTHIA [pythia] with the CTEQ6L [cteq] parton distribution functions (PDF). Events are reweighted by the ratio of next-to-next-to-leading order to leading-order cross sections as a function of dimuon mass [carena]. We use the standard CDF simulation [cdfsim] to model the detector response to the particles in the event. The overall normalization of this background is derived from data near the Z boson pole mass, $70 < M_{\mu\mu} < 110 \text{ GeV}/c^2$.

The remaining background contributions are small relative to standard model sources of dimuons. Decays of WW (1%) and $t\bar{t}$ (1%) to dimuons are described using PYTHIA and the CDF detector simulation, normalized

to NLO cross sections [ttandw]. The background from objects misidentified as muons (0.5%) is estimated using the distribution of calorimeter energy in the vicinity of each candidate muon in the sample [topdil]. Cosmic ray backgrounds (<0.01%) are modeled using identified cosmic ray events, weighted by the probability to survive the cosmic ray removal algorithm [cosmics].

The observed spectrum of dimuon invariant mass ($M_{\mu\mu}$) is in good agreement with the total SM plus cosmic-ray prediction, as shown in Fig. 1. We expect 1851 ± 90 events with $M_{\mu\mu} > 130$ GeV/ c^2 , and observe 1813 events.

We model the production and decay of a spin-1 resonance Z'_{SM} using MADEVENT [madgraph], assuming fermionic couplings equal to those of the Z boson. Initial-state QCD radiation, hadronization, and showering are modelled with PYTHIA. The acceptance for Z' boson events varies with mass, increasing from 20% at 200 GeV/ c^2 to nearly 40% at 1 TeV/ c^2 , then dropping for $M_{Z'} > 1$ TeV/ c^2 due to lack of initial-state partons with sufficient momentum.

(error|bad image|null box)(error|bad image|null box)

FIG. 1. Top: The distributions of $M_{\mu\mu}$ for data with 4.6 fb^{-1} of integrated luminosity (triangles) and expected SM backgrounds (histograms) with two example Z'_{SM} signals. Bottom: The relative difference between observed and expected data, as a function of dimuon mass. Error bars show statistical uncertainty.

The previous CDF search [zprimetemp] used a binned likelihood fit with bins uniform in the inverse of the reconstructed dimuon mass to extract the best-fit signal cross section at a range of masses. That approach weighted events in the same reconstructed inverse mass bin equally, independent of expected track resolutions. We improve on this method by using an unbinned likelihood that includes a theoretical model of the full kinematics of the event and the event-by-event knowledge of the muon p_T resolution. Well-measured events have narrower likelihoods, reflecting the higher quality of their information and making a stronger impact on the fitted result. The likelihood is then used both to set limits on the Z' cross section as a function of mass and to construct a 2D interval that gives a well-defined discovery condition. The likelihood is given by

$$L(M_{Z'}, s_{Z'}) = \frac{(N_{bg+Z'})^N e^{-(N_{bg+Z'})}}{N!} \prod_i^N L(x_i | M_{Z'}, s_{Z'}),$$

where $M_{Z'}$ is the Z' pole mass, N is the number of events in the data, $N_{bg, Z'}$ are the number of events due to background and Z' signal, x_i represents the observed kinematics of the i -th event, and $s_{Z'} = N_{Z'} / (N_{bg} + N_{Z'})$. The dependence of the per-event likelihood is given by

$$L(x_i | M_{Z'}, s_{Z'}) = s_{Z'} L_{Z'}(x_i | M_{Z'}) + (1 - s_{Z'}) L_{Z/\gamma^*}(x_i),$$

and the likelihood $L_{Z'}$ is calculated by integrating the matrix element for Z' production convolved with PDFs and the detector resolution functions:

$$\begin{aligned} L_{Z'}(x_i = p_1, p_2, \sigma_{p_{T1}}, \sigma_{p_{T2}}, N_{\text{jets}} | M_{Z'}) = \\ \int d\Phi(q_1, q_2) |\mathcal{M}_{Z'}(q_1, q_2, M_{Z'})|^2 f_{PDF}^p f_{PDF}^{\bar{p}} \\ \times \times T(p_1, q_1, \sigma_{p_{T1}}) T(p_2, q_2, \sigma_{p_{T2}}) \times P_{PT}(q_1 + q_2, N_{\text{jets}}), \end{aligned}$$

where $p_{1,2}$ represent the four-vectors of the two measured muons, $q_{1,2}$ represent the unknown four-vectors of the two true muons, Φ represents phase space for the true muons, \mathcal{M} is the matrix element, f_{PDF} is the parton distribution function, $T(p, q, \sigma_{p_T})$ is the transfer function that parametrizes the detector resolution as a function of the measured uncertainty σ_{p_T} , and P_{PT} is the probability density function for p_T of the $\mu\mu$ system, parameterized in the number of jets (N_{jets}) with $E_T > 15$ GeV and $|\eta| < 2.5$. The distributions of σ_{p_T} for the Z' signal and dominant Z/γ^* background are the same in the phase space region near the hypothesized Z' mass, thus they do not affect the likelihood ratio ordering. The distribution of P_{PT} is obtained from simulated samples with initial- and final-state radiation. An analogous expression is used for L_{Z/γ^*} , which describes the likelihood for the dominant Z/γ^* background.

We analyze the resulting likelihood in two ways. First, we aim to discover the regions in $(M_{Z'}, s_{Z'})$ that are consistent with the data and inconsistent with the SM, making no assumptions about the relationship between $M_{Z'}$ and $s_{Z'}$. We refer to this as the *2D interval* analysis. Second, we wish to set limits on the Z' mass in specific models. In that case, we perform a *raster scan*, in which we choose a set of values of $M_{Z'}$, and at each point derive limits on $s_{Z'}$. Together with a prediction for $s_{Z'}(M_{Z'})$ in a specific theory, we can use the raster scan to place lower limits on $M_{Z'}$.

The 2D interval is constructed via the unified ordering scheme [feldcous] in two dimensions, resonance mass and cross section (see Fig. 3). At each test point in the $(M_{Z'}, s_{Z'})$ space, we calculate the ratio of the likelihood at the test point to the likelihood at the best-fit point where the likelihood is maximized. To determine which test points are consistent with the data at a given confidence level, we perform pseudo-experiments to determine how often we expect to observe such a likelihood ratio. The pseudo-experiments include all backgrounds and interference effects between the Z and Z' , as well as variation of the nuisance parameters from systematic uncertainties described below. This approach is well designed for discovery, as it tests the background hypothesis exactly once. The significance of an observation corresponds to the first confidence-level

contour that includes a signal rate of zero. It also provides a summary of Z' models consistent with the data without relying on specific model details. In the 2D interval analysis, the best-fit signal cross section of $\sigma = 26$ fb occurs at a resonance mass of $M = 199$ GeV/ c^2 , but is consistent with zero at 16% confidence level.




FIG. 2. Observed 95% CL limits in 1D raster scan (top) and 2D intervals (bottom) for data with 4.6 fb^{-1} of integrated luminosity. The solid circle indicates the best-fit value and the lines define regions in which 25, 50, 68, 95, and 99% of experiments would yield results less consistent with the standard model and the data.

The raster scan is the traditional approach used in many analyses, including the previous Z' search [zprimetemp]. It provides mass limits on theories that enforce a relationship between the signal fraction and the resonance mass, and is appropriate if outside information indicates a particular mass is interesting. In the presence of a significant excess above the background-only hypothesis, one must account for the number of possible Z' masses, each of which tests the background-only hypothesis: the *look-elsewhere effect*. The 2D analysis needs no such correction. While the resulting discovery significance of the corrected raster scan will be correct, one will still be left with an interval in the signal fraction at every mass. In contrast, in the presence of a signal, the 2D analysis will provide a range of masses that is consistent with the signal.

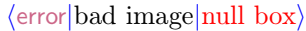


FIG. 3. Observed 95% CL limits for data with 4.6 fb^{-1} of integrated luminosity expressed as limits on the up and down type charges c_u and c_d [carena]. The solid and dotted lines show possible models in $U(1)_{B-XL}$ and $U(1)_{10+x5}$ groups, respectively. The dashed lines show the range for models in the $U(1)_{q+xu}$ group.

down-type fermions to the $U(1)$ group associated with the Z' . Table II shows the limits for the specific models described in Ref [carena].

In conclusion, we have applied the matrix-element-based likelihood technique to a search for new spin-1 resonances decaying to muon pairs, set the strongest limits to date on the resonance cross section and mass, and introduced a statistical analysis approach that is useful for this analysis as well as for potential LHC discoveries.

ACKNOWLEDGMENTS

We acknowledge useful conversations with Tim Tait. We thank the Fermilab staff and the technical staffs of the participating institutions for their vital contributions. This work was supported by the U.S. Department of Energy and National Science Foundation; the Italian Istituto Nazionale di Fisica Nucleare; the Ministry of Education, Culture, Sports, Science and Technology of Japan; the Natural Sciences and Engineering Research Council of Canada; the National Science Council of the Republic of China; the Swiss National Science Foundation; the A.P. Sloan Foundation; the Bundesministerium für Bildung und Forschung, Germany; the World Class University Program, the National Research Foundation of Korea; the Science and Technology Facilities Council and the Royal Society, UK; the Institut National de Physique Nucleaire et Physique des Particules/CNRS; the Russian Foundation for Basic Research; the Ministerio de Ciencia e Innovación, and Programa Consolider-Ingenio 2010, Spain; the Slovak R&D Agency; and the Academy of Finland.

TABLE II. Mass limits on specific spin-1 Z' models [carena] with 4.6 fb^{-1} of integrated luminosity at 95% confidence level.

Model	Z'_l	Z'_{sec}	Z'_N	Z'_ψ
Mass Limit (GeV/ c^2)	817	858	900	917

Dominant systematic uncertainties [zprimetemp] include uncertainties on the PDFs and the dependence of the next-to-leading order cross section on the dimuon invariant mass. These weaken the final limits by 5-10% depending on mass. Additional uncertainties are the level of initial state radiation and muon acceptance at large transverse momentum.

The raster scan in mass allows us to set strong limits on specific models of Z' production; see Fig. 3 and Table II. The production cross section times branching fraction to the dimuon final state is determined by the couplings of the fermions to the Z' . Figure 3 shows how mass limits depend on the charges of the up- and

[Langacker] P. Langacker, Rev. Mod. Phys. **81**, 1199 (2009), and references therein. [littlehiggs] N. Arkani-Hamed, A. G. Cohen, and H. Georgi, Phys. Lett. B **513**, 232 (2001); T. Han, H. E. Logan, B. McElrath and L.-T. Wang, Phys. Rev. D **67**, 095004 (2003); T. Han, H. E. Logan, and L.-T. Wang, J. High Energy Phys. **01**, 099 (2006); M. Perelstein, Prog. Part. Nucl. Phys. **58**, 247 (2007). [nmssm] M. Cvetič and P. Langacker, Phys. Rev. D **54**, 3570 (1996); M. Cvetič *et al.*, Phys. Rev. D **56**, 2861 (1997); E. Keith and E. Ma, Phys. Rev. D **56**, 7155 (1997); P. Langacker and J. Wang, Phys. Rev. D **58**, 115010 (1998). [zprimetemp] T. Aaltonen *et al.* (CDF Collaboration), Phys. Rev. Lett. **102**, 091805 (2009). [d0ee] V. Abazov *et al.* (D0 Collaboration), arXiv:1008.2023v1 (2010). [cdfee] T. Aaltonen *et al.* (CDF Collaboration), Phys. Rev. Lett. **102**, 031801 (2009).

- [cdf]** D. E. Acosta *et al.* (CDF Collaboration), Phys. Rev. D **71**, 032001 (2005); A. Abulencia *et al.* (CDF Collaboration), J. Phys. G **34**, 2457 (2007); T. Aaltonen *et al.* (CDF Collaboration), Phys. Rev. D **77**, 112001 (2008).
- [coordinates]** CDF uses a cylindrical coordinate system with the z axis along the proton beam axis. Pseudorapidity is $\eta \equiv -\ln(\tan(\theta/2))$, where θ is the polar angle relative to the proton beam direction, and ϕ is the azimuthal angle while $p_T = |p|\sin\theta$, $E_T = E\sin\theta$.
- [cteq]** J. Pumplin *et al.* (CTEQ Collaboration), J. High Energy Phys. 07 (2002) 012.
- [carena]** M. Carena, A. Daleo, B. A. Dobrescu, and T. M. P. Tait, Phys. Rev. D **70**, 093009 (2004).
- [cdfsim]** T. Affolder *et al.* (CDF Collaboration), Nucl. Instrum. Methods **A447**, 1 (2000).
- [ttandww]** J. M. Campbell and R. K. Ellis, Phys. Rev. D **60**, 113006 (1999); R. Bonciani, S. Catani, M. L. Mangano, and P. Nason, Nucl. Phys. B **529**, 424 (1998); M. Cacciari *et al.*, J. High Energy Phys. 04 (2004) 068.
- [cosmics]** A. V. Kotwal, H. K. Gerberich, and C. Hays, Nucl. Instrum. Methods Phys. Res., Sect. A **506**, 110 (2003).
- [topdil]** D. Acosta *et al.* (CDF Collaboration), Phys. Rev. Lett. **93**, 142001 (2004).
- [madgraph]** J. Alwall *et al.* J. High Energy Phys 07 (2007) 028
- [pythia]** T. Sjöstrand *et al.*, Comput. Phys. Commun. **135** (2001) 238 T. Sjöstrand, Comput. Phys. Commun. **82**, 74 (1994).
- [feldcous]** G. J. Feldman and R. D. Cousins, Phys. Rev. D **57**, 3873 (1998).